# Single-Filter Multi-Color CMOS Fluorescent Contact Sensing Microsystem

Derek Ho[1], M. Omair Noor[2], Ulrich J. Krull[2], Glenn Gulak[1], and Roman Genov[1]
[1]Department of Electrical and Computer Engineering, University of Toronto
[2]Department of Chemical and Physical Sciences, University of Toronto Mississauga

***Abstract*— A multi-color fluorescent contact sensing microsystem is presented. The microsystem employs a CMOS field-modulated color sensor (FCS) to spectrally detect and differentiate among multiple emission bands, requiring only one on-CMOS longpass filter. A FCS prototype has been fabricated in a standard 0.35$\mu$m CMOS technology. The multi-color imaging capability of the FCS microsystem has been validated in the detection of green-emitting and red-emitting quantum dots (QDs) with QD concentration detection limits of 313nM and 78nM, respectively.**

## I. Introduction

Fluorescence imaging has become a popular methodology to discriminate between multiple proteins, organelles, or functions in an organism [1]. This imaging technique is invaluable to many areas of the life sciences, in particular, to DNA analysis for pathogen detection and cancer diagnostics [2].

For applications involving DNA detection, fluorescence is a commonly used transduction method to interrogate a nucleic acid hybridization event, where single-stranded target DNA strands (to be identified) are labelled with fluorescent markers such as an organic fluorophore dye [3]. The extent of hybridization is then determined by quantifying the emission from fluorescent markers.

Despite the prominence of the microarray technology, where DNA probes are spatially registered onto a planar array, there are drawbacks [3]. Typically microarrays are expensive to manufacture and are laboratory-based in terms of energy and material requirements. They also offer a much greater capability, such as parallelism, than most often required.

To concurrently analyze multiple targets without the need for spatially registering immobilized probes, different DNA target sequences can be associated with different fluorescent markers, for example quantum dots (QDs), that can be distinguished using emission wavelength channels, hence allowing wavelength multiplexing to simultaneously determine different nucleic acid targets. QDs have a number of unique optical properties that make them useful for multiplexing. These properties include broad excitation spectra, greater resistance to photobleaching than organic fluorophores, larger Stokes shifts (>100nm) and size-tunable narrow and symmetrical emission spectra.

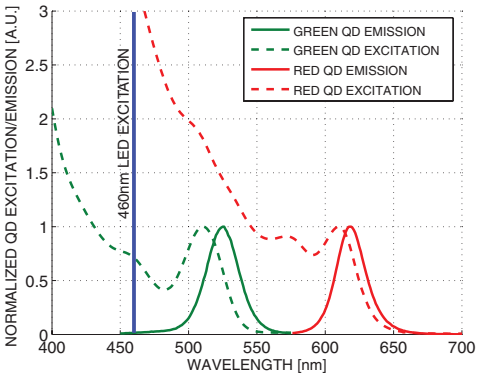


Fig. 1: Fluorescent excitation and emission spectra of quantum dots.

Multi-color fluorescence imaging utilizes markers that absorb light and emit at longer and well-separated wavelengths, typically between 500nm to 700nm, such as shown in Fig. 1. Therefore, unlike other spectroscopic techniques, such as Raman spectroscopy, where continuous fine spectral resolution is required, fluorescent imaging requires spectral differentiation among several discrete wavelengths.

The fluorescent microscope is the most commonly used equipment for fluorescent imaging. However it is bulky and expensive. Unlike the conventional fluorescent microscope, in contact imaging the object to be imaged is placed in close proximity to the focal plane, eliminating the need for bulky and expensive optics such as a system of lenses and mirrors, which enables miniaturized detectors to realize a lab-on-a-chip platform.

Conventionally, color separation has been achieved by using a set of optical bandpass filters to select different parts of the emission spectrum. The optics involved is bulky and expensive, and the mechanical swapping of filters prevents parallelization of this process. Methods based on diffraction grating (the splitting of light) [4] and Fabry-Perot etalon (tuned resonance cavity) [5] generally offer high spectral resolution, but

978-1-4673-0219-7/12/$31.00 ©2012 IEEE

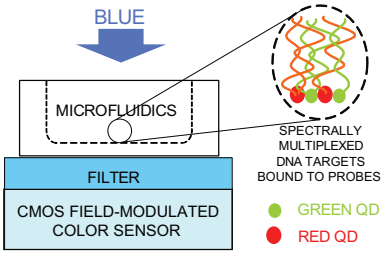


Fig. 2: CMOS fluorescent contact sensing microsystem.

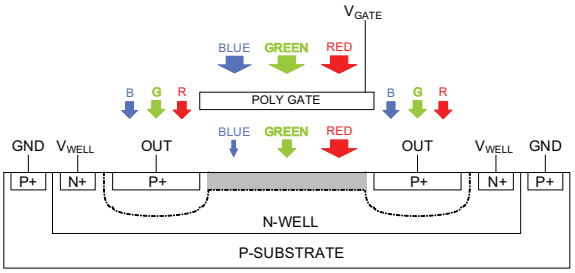


Fig. 3: Field-modulated color detector (FCD).

require micromachining and post-processing such as wafer polishing and wafer bonding. Eliminating the need for sophisticated optics and post-processing is the ultimate remedy to high design complexity and fabrication cost.

Techniques that solely rely on integrated circuit process technology have been developed, most notably the buried junction technology [6] (which the Foveon sensor is based on). Since light absorption in a semiconductor varies across wavelengths in such a way that light of a longer wavelength can penetrate deeper, a photocurrent measured at a deeper depth consists of stronger long-wavelength components. By sensing at several depths, color information can be inferred. Although the buried junction approach achieves high spatial density and is suitable for photographic applications requiring only three colors (e.g., red, green, and blue), there is a limit to the number of diodes that can be implemented. This renders it unsuitable for applications that require sensing at more than three wavelengths. To overcome this limitation, a spectrally-sensitive photodiode that can potentially sense more than three colors has been reported [7]. A biased polysilicon gate modulates the photo sensing region depth to effectively achieve an equivalent of many buried diodes. However, the reliance on sensing at multiple depths along the vertical dimension limits scalability. The most recently reported prototype is fabricated in a 5$\mu$m custom process [7].

In this paper, we present a low-cost multi-color CMOS fluorescent contact sensing microsystem. The core of the microsystem depicted in Fig. 2 is a CMOS field-modulated color sensor (FCS) to spectrally detect quantum dot emission bands and differentiate among them. Only one additional on-CMOS optical filter to reject the excitation light is required. The FCS is prototyped in a standard digital 0.35$\mu$m CMOS technology with an on-chip analog-to-digital converter.

## II. Device and Circuit Implementation

When multiple wavelengths of light are incident simultaneously, the intensities at these wavelengths can be determined by measurements from multiple photo detectors of unique spectral response [8]. For example, for a two-wavelength input, the photo currents $I_1$ and $I_2$ measured by two photo detectors can be related to the input intensities $\phi_1$ and $\phi_2$ by

$$I_1 = k_{11}\phi_1 + k_{12}\phi_2 \quad (1)$$

$$I_2 = k_{21}\phi_1 + k_{22}\phi_2 \quad (2)$$

where the $k$-parameters describe the transfer function of the detectors and can be obtained empirically. The input intensities $\phi_1$ and $\phi_2$ can be obtained by solving the system of equations, provided that the detectors have unique spectral responses (i.e. each equation must be linearly independent). This model can be extended to a finite set of $N$ wavelengths. To determine the intensity of an input spectrum to a resolution of $N$ distinct wavelengths, $N$ measurements are required from each of $N$ detectors.

To create the equivalent of multiple photo detectors with unique spectral response, the field-modulated color detector (FCD) depicted in Fig. 3 has been implemented. The four-terminal device consists of several concentric ring structures including a p+ diffusion ring (detector output) and an n+ diffusion ring (well bias) in an n-well, surrounded by a p+ diffusion ring (substrate bias) on the p-type substrate. The polycrystalline silicon gate functions as both an optical filter and a gate bias terminal for spectral response modulation. The p+ output diffusion is set to a voltage close to ground by an external circuit. The n-well is biased at a voltage higher than the p+ diffusion to form a reverse biased junction.

When a high gate bias $V_{GATE}$ is applied such that no depletion region is formed under the gate, photo detection only takes place at the p+/n-well depletion region. Photo-generated minority carrier holes in the n-well within one diffusion length from the depletion region drift across the depletion region and are collected by the p+ region, which is at the lowest voltage. Excess majority carrier electrons in the n-well are discharged through the well contact.

When a low voltage is applied to the gate, majority carrier electrons in the n-well are repelled from the silicon surface and a depletion region is formed. This depletion region also participates in photo detection,

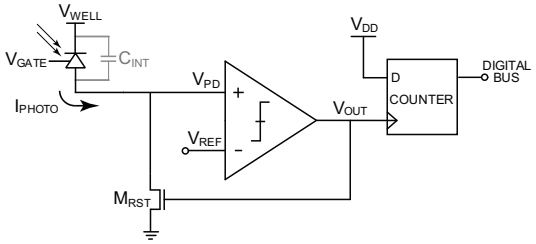


Fig. 4: Field-modulated color sensor circuit.

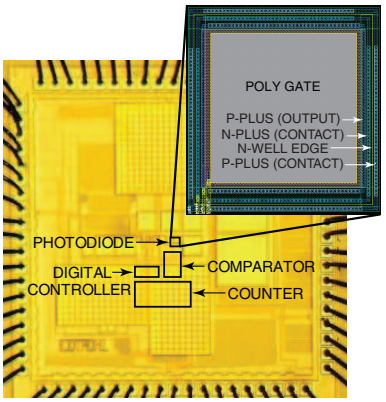


Fig. 5: Chip micrograph of the 2mm×2mm FCS with a 50$\mu$m×50$\mu$m FCD in 0.35$\mu$m standard CMOS.

but the light experiences wavelength-dependent absorption as it travels through the gate. Since the gate provides greater attenuation at shorter wavelengths, the sensing region under the gate provides additional long-wavelength (e.g., red) responsivity to the FCD. Since the peripheral and central portions of the FCD yield different spectral properties, when different gate voltages are applied, the equivalent of multiple detectors with unique spectral responses is created, implementing (1) and (2) for two gate voltages in a single device.

The absorption characteristic of the poly gate deserves further discussion. In polysilicon, light is absorbed exponentially as a function of penetration depth [9]. Transmitted light $T$ after passing silicon with thickness $x$ can be approximated as $T = e^{-\alpha x}$ where $\alpha$ is the wavelength-dependent absorption coefficient, with values 3.56, 1.35, and 0.45$\mu$m$^{-1}$ for the wavelengths of 460nm (blue), 520nm (green), and 620nm (red), respectively [9].

Although the gate thickness is typically a fixed parameter for a process, it is interesting to note a tradeoff in gate thickness. A thicker gate translates to a greater difference in spectral properties between the periphery and center of the FCD, which is essential for spectral selectivity, at the expense of less light reaching the center of the detector. For example, for a 0.35$\mu$m CMOS process, the thickness of the polysilicon gate is around 250nm [10], leading to an approximate attenuation of 60% for blue light (460nm), 30% for green light (520nm), and 10% for red light (620nm).

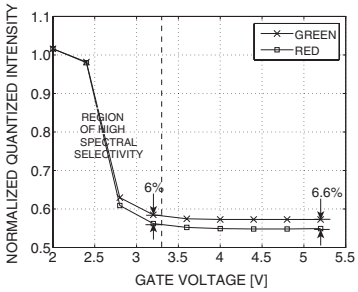


Fig. 6: Measured photo response of the FCS normalized at $V_{GATE}$ = 2V.

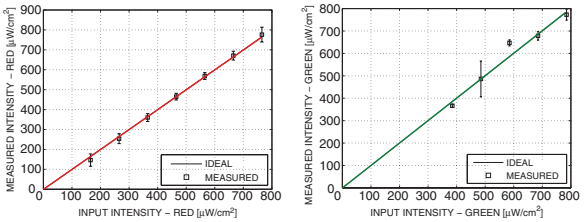


(a) (b)

Fig. 7: Measured intensity: (a) 640nm, and (b) 540nm.

The overall FCS circuit is depicted in Fig. 4. The FCS converts the photocurrent generated by the FPD to a 16-bit digital output, which is then fed into a reconstruction software script that solves for the input spectrum $\phi$. The FCS is implemented using a current-to-frequency ADC that measures the light intensity by counting the number of resets during the integration time [11]. It is insensitive to supply voltage scaling as it removes the voltage headroom constraint by representing light intensity in the temporal domain.

## III. Measurement Results

Fig. 5 depicts the micrograph of the prototype FCS, with a 50$\mu$m×50$\mu$m FCD, implemented in a 0.35$\mu$m standard CMOS technology. It has been tested in light intensity measurements at the red (640nm) and green (540nm) wavelengths. Two current-controlled light-emitting diodes (LEDs) provide input illumination. Fig. 6 depicts the measured photo response of the FCS across gate voltages for red and green light. For a $V_{GATE}$ change from 2V to 5.2V and $V_{WELL}$ of 2V, the change in the photocurrent for red illumination is 6.6% less than that for green illumination. The FCS spectral selectivity is based on this difference and is most prominent between the $V_{GATE}$ of 2V to 3.3V (6%). For FCS operation within the nominal supply voltage, $V_{GATE}$ of 2V and 3.3V are chosen for the two field-modulation settings.

Fig. 7 depicts measured intensities for an illumination that simultaneously contains light power at 640nm (red) and 540nm (green), computed using equations (1)

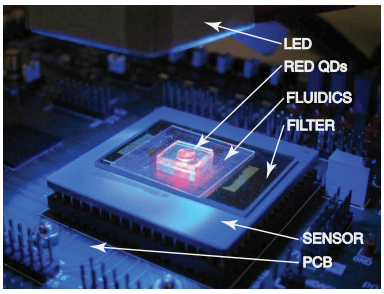


Fig. 8: Photograph of the microsystem test setup.

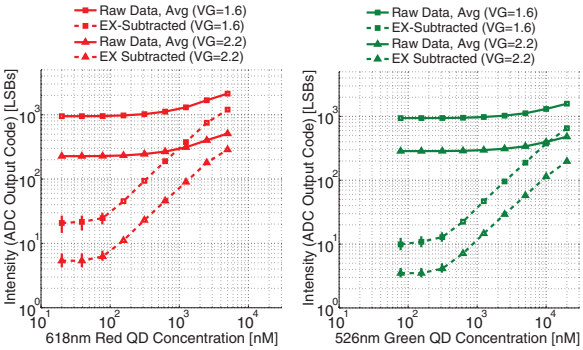


Fig. 9: Measured calibration curves: (a) rQDs, and (b) gQDs.

and (2). Fig. 7(a) and (b) depict measured red intensity and green intensity, respectively, with each data point containing a sweep across all intensities of the other color. The error bars depict a range of one standard deviation away from the mean value.

Fig. 8 is a photograph of the prototyped contact sensing microsystem. The microsystem has been verified through the detection of red-emitting QDs (rQDs) and green-emitting QDs (gQDs) with absorption and emission spectra depicted in Fig. 1. QDs are imaged in a reservoir made from polydimethylsiloxane (PDMS) and glass. The excitation (460nm LED) is directed through an OD2 rejection filter (480nm long-pass) to attenuate the excitation light intensity.

The calibration curves for rQDs and gQDs are depicted in Fig. 9(a) and (b), respectively. Background subtraction has been performed to remove residue excitation (EX). Each error bar denotes one standard deviation based on eight measurements. Error bars are included for all data on the EX-subtracted curves but in some cases are too small to be visible. Detection limits are found to be 313nM and 78nM for gQD and rQD, respectively. The difference in the detection limits is because of the fact that rQDs are brighter than gQDs for a given concentration due to the larger extinction coefficient of rQDs.

Detection using multiple FCD gate voltages enables spectral sensing. For each quantum dot concentration, two measurements, $I(V_{GATE1})$ and $I(V_{GATE2})$, are performed at two gate voltages ($V_{GATE1} = 1.6V$, $V_{GATE2} = 2.2V$, for $V_{WELL}$ biased at $1.6V$). The ratio of the photo currents, $I(V_{GATE1})/I(V_{GATE2})$, is wavelength-dependent. The ratios are 3.3 and 4.2 for gQDs and rQDs, respectively, and provide a means to differentiate the quantum dot emissions.

TABLE I: EXPERIMENTAL CHARACTERISTICS

| | |
|---|---|
| Technology | 0.35$\mu$m CMOS |
| Supply Voltage | 3.3V |
| Power Consumption | 0.3mW |
| Pixel Size | 50$\mu$m x 50$\mu$m |
| Optical Sensitivity | 1$\mu$W/cm$^2$/level |
| Dark Current | 0.25 count/sec |
| Max. Pulse Frequency | 10MHz |

## IV. Conclusion

A microsystem for multi-color fluorescent contact sensing is presented. The microsystem includes a field-modulated color sensor that detects and differentiates among the emissions of red and green quantum dots at the nano-molar concentration level without the use of red or green optical filters. The entire detection system utilizes only one filter for excitation rejection and is scalable to an arrayed implementation, enabling low-cost, high-throughput, and miniaturized biosensors.

## References

[1] H. Ai, K. Hazelwood, M. Davidson, and R. Campbell, "Fluorescent protein FRET pairs for ratiometric imaging of dual biosensors," *Nature Methods*, vol. 5, no. 5, pp. 401–403, 2008.

[2] X. Gao, Y. Cui, R. Levenson, L. Chung, and S. Nie, "In vivo cancer targeting and imaging with semiconductor quantum dots," *Nature Biotechnology*, vol. 22, no. 8, pp. 970–976, 2004.

[3] M. Schena, D. Shalon, R. Davis, and P. Brown, "Quantitative monitoring of gene expression patterns with a complementary DNA microarray," *Science*, vol. 270, no. 5235, Oct 1995.

[4] S. Kong, D. Wijngaards, and R. Wolffenbuttel, "Infrared micro-spectrometer based on a diffraction grating," *Sensors and Actuators A*, no. 92, pp. 88–95, 2001.

[5] J. Correia, G. Graaf, M. Bartek, and R. Wolffenbuttel, "A single-chip CMOS optical microspectrometer with light-to-frequency converter and bus interface," *IEEE J. Solid-State Circuits*, vol. 37, no. 10, pp. 1344–1347, Oct 2002.

[6] X. Fang, V. Hsiao, V. Chodavarapu, A. Titus, and A. Cartwright, "Colorimetric porous photonic bandgap sensors with integrated CMOS color detectors," *IEEE Sensors Journal*, vol. 6, no. 3, pp. 661–667, Jun 2006.

[7] H. Ishii, Y. Maruyama, H. Takao, M. Ishida, and K. Sawada, "Improvement in filter-less fluorescence sensor capability by optimization of potential distribution," *4th Asia-Pacific Conf. on Transducers and Micro-Nano Tech.*, pp. 68–71, Jun 2008.

[8] A. Belouchrani, K. Abed-Meraim, J. Cardoso, and E. Moulines, "A blind source separation technique using second-order statistics," *IEEE Trans. Signal Processing*, vol. 45, no. 2, 1997.

[9] S. Dimitrijev, *Principles of semiconductor devices*, 1st ed. Oxford University Press, 2006.

[10] H. Wong, "Technology and device scaling considerations for CMOS imagers," *IEEE Trans. on Electron Devices*, vol. 43, no. 12, pp. 2131–2142, Dec 1996.

[11] D. Ho, G. Gulak, and R. Genov, "CMOS field-modulated color sensor," in *IEEE Custom Integrated Circuit Conf.*, Sep 2011.